

# 光学学报

## 微波光子信道化链路非线性失真的数字补偿方法

王锦成, 陈萧恩, 丁玟, 陈建平, 吴龟灵\*

上海交通大学区域光纤通信网与新型光通信系统国家重点实验室, 上海 200240

**摘要** 微波光子信道化链路的线性度主要受信道内的交调失真和信道间的互调失真的限制。本文提出了一种基于数字域迭代的非线性失真补偿方法, 对各个信道输出的中频信号在数字域进行联合处理, 通过迭代不断逼近线性化的理想结果, 能够同时有效抑制信道化链路中的交调失真和互调失真。仿真结果表明, 在参数无偏差的情况下, 该方法可以完全抑制信道内的交调失真和信道间的互调失真; 在参数偏差为 5% 的情况下, 仍可以将三阶交调失真和互调失真分别抑制 15 dB 和 16 dB。

**关键词** 傅里叶光学与信号处理; 交调失真; 互调失真; 微波光子; 数字信号处理

中图分类号 TN911.7 文献标志码 A

DOI: 10.3788/AOS222132

### 1 引言

随着信息时代的到来, 电子对抗、多业务宽带接入以及卫星导航等技术都向着高频段、大带宽的趋势发展。受制于电子瓶颈<sup>[1-2]</sup>, 传统的微波器件已经不能满足以上性能需求。微波光子信道化技术<sup>[3-5]</sup>将宽带信号转换到光域进行处理, 通过频谱切割将其分解成多个窄带信号, 并下变频到低频段, 分别进行检波和信号处理, 突破了传统微波器件在工作频段和带宽上的限制。目前, 微波光子信道化链路大多使用基于电光调制器的外调制技术。由于电光调制器固有的余弦响应, 射频信号在调制到光上的过程会产生谐波失真、信道内的交调失真(IMD), 以及信道间的互调失真(XMD)。谐波失真可以通过滤波器有效地去除, IMD 和 XMD 便成了制约系统性能的主要因素。传统的微波光子窄带链路<sup>[6]</sup>主要受三阶交调失真(IMD3)的限制, 已经提出多种线性化方案来解决这个问题, 如前馈补偿<sup>[7-8]</sup>、电的预失真<sup>[9-10]</sup>、双平行电光调制<sup>[11-12]</sup>, 以及数字信号处理<sup>[13-14]</sup>等。文献[14]在数字域利用迭代算法, 不仅抑制了 IMD3, 还抑制了信道内的高阶 IMD。但是不能抑制信道间的 XMD。文献[15]通过预失真电路消除了多个信道间的 XMD, 但系统仍然受到 IMD3 的限制。文献[16]同时抑制了 IMD3 和 XMD, 但需要额外的链路提取失真信息, 增加了系统的复杂度。文献[17]通过反转链路的传递函数在数字域实现了 IMD3 和 XMD 的同时补偿。但该算法对输入信号功率的范围有限制, 补偿效果随输入信号功率增加而下降。文献[18-19]引入人工神经网络到后端数字信

号处理的过程中, 但该类方案往往需要复杂的网络结构设计和大量的数据预训练。

针对信道化相干探测链路中的 IMD 和 XMD 的问题, 本文提出一种基于数字域迭代的非线性失真补偿方法。该方法不需要构建复杂的补偿函数模型, 或者引入额外的硬件设备, 只需要在后端数字信号处理模块提取各信道内的信号, 进行联合处理, 便可同时抑制信道内的 IMD 和信道间的 XMD。仿真结果表明, 在参数无偏差的情况下, 该方法只需要几次迭代即可完全抑制信道内的 IMD 和信道间的 XMD; 在参数偏差为 5% 的情况下, IMD3 和 XMD 分别改善了 15 dB 和 16 dB。

### 2 基本原理

图 1 为等效的微波光子信道化相干接收原理示意图。激光器输出的连续光通过马赫-曾德尔调制器(MZM)调制上宽带微波信号, 在光域上完成信道划分。每个信道只保留正(或负)一阶光边带, 并将其与相应的本振光进行相干探测, 由平衡探测器输出中频信号。经过模数转换器后送入数字信号处理单元进行联合处理补偿非线性失真, 恢复接收的信号。

信道化接收的宽带微波信号由多个不同中心频率(子载波)的子带信号组成<sup>[17,20]</sup>, 可以表示为

$$X(t) = \sum_k A_k(t) \sin [\omega_k t + \varphi_k(t)], \quad (1)$$

式中,  $\omega_k$ 、 $A_k(t)$  和  $\varphi_k(t)$  分别为第  $k$  个子带信号的中心频率、包络振幅和相位。当各信道子载波的谐波项和相互耦合产生的交调项不落入任一个信道时, 第  $k$  个

收稿日期: 2022-12-12; 修回日期: 2023-02-20; 录用日期: 2023-03-07; 网络首发日期: 2023-03-13

通信作者: \*wuguling@sjtu.edu.cn

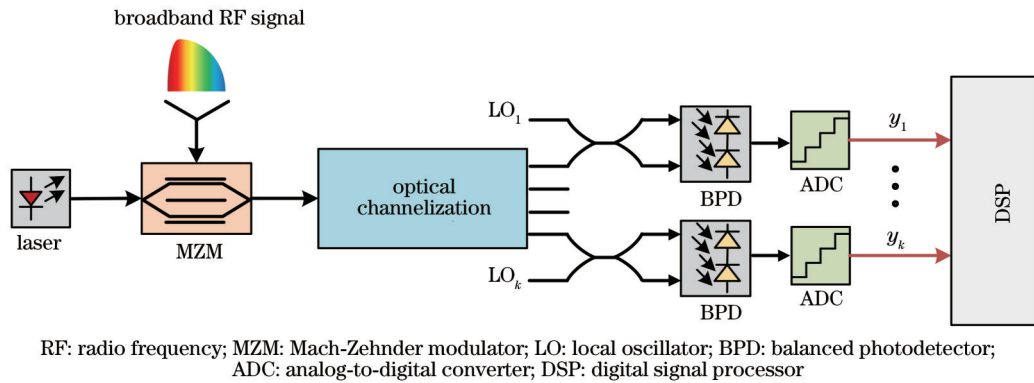


图1 微波光子信道化相干接收原理示意图

Fig. 1 Schematic diagram of a microwave photonic channelized coherent reception

信道输出的中频信号<sup>[16-17]</sup>可以表示为

$$y_k = g_k \times \prod_{p \neq k} J_0[\beta A_p(t)] \times J_1[\beta A_k(t)] \times \sin[\omega_{\text{IF}} t + \varphi_k(t)], \quad (2)$$

式中:  $\beta = \pi / V_\pi$  ( $V_\pi$  是调制器的半波电压);  $J_n(x)$  是  $n$  阶第一类贝塞尔函数;  $\omega_{\text{IF}}$  是中频信号的频率;  $g_k$  是一个常数, 与第  $k$  个信道光子链路的增益有关。对式(2) 进行泰勒展开, 可以得到:

$$y_k \approx \frac{g_k}{2} \left( \overbrace{\beta A_k(t)}^{\text{1st}} - \underbrace{\frac{\beta^3 A_k^3(t)}{8} + \frac{\beta^5 A_k^5(t)}{192} - \dots}_{\text{IMD}} \right) \sin[\omega_{\text{IF}} t + \varphi_k(t)] \times \prod_{p \neq k} \left( 1 - \frac{\overbrace{\beta^2 A_p^2(t)}^{\text{XMD}} + \frac{\beta^4 A_p^4(t)}{64} - \dots}{4} \right). \quad (3)$$

式(3)中包含  $A_k(t)$  的高次项代表信道内的 IMD, 如 IMD3、五阶 IMD(IMD5)等, 包含  $A_p(t)$  的多项式代表信道间的 XMD。理想的中频信号仅仅包含其中的基频项, 可以表示为

$$\tilde{y}_k = \frac{g_k}{2} \beta A_k(t) \sin[\omega_{\text{IF}} t + \varphi_k(t)]. \quad (4)$$

由式(3)、式(4)可得

$$\frac{y_k}{\tilde{y}_k} = \sum_{m=0}^{\infty} \frac{(-1)^m}{m!(m+1)!} \left( \frac{1}{2} \right)^{2m} \left\{ [\beta A_k(t)]^2 \right\}^m \times \left\{ \sum_{n=0}^{\infty} \frac{(-1)^n}{n! n!} \left( \frac{1}{2} \right)^{2n} \left\{ [\beta A_p(t)]^2 \right\}^n \right\}. \quad (5)$$

式(5)中的  $[\beta A_k(t)]^2$  ( $k=1, 2, \dots$ ) 可表示为<sup>[14]</sup>

$$[\beta A_k(t)]^2 = 2 \left\langle \left[ \beta A_k(t) \sin[\omega_{\text{IF}} t + \varphi_k(t)] \right]^2 \right\rangle = \frac{8}{g_k^2} \langle \tilde{y}_k^2 \rangle, \quad (6)$$

式中,  $\langle \cdot \rangle$  为低通滤波。由此可得以下数学关系:

$$\begin{aligned} \tilde{y}_k &= \frac{y_k}{\sum_{m=0}^{\infty} \frac{(-1)^m}{m!(m+1)!} \left( \frac{1}{2} \right)^{2m} \left[ \frac{8}{g_k^2} \langle \tilde{y}_k^2 \rangle \right]^m \times \prod_{p \neq k} \left\{ \sum_{n=0}^{\infty} \frac{(-1)^n}{n! n!} \left( \frac{1}{2} \right)^{2n} \left[ \frac{8}{g_p^2} \langle \tilde{y}_p^2 \rangle \right]^n \right\}} = \frac{y_k}{\Gamma_{m,k}[\langle \tilde{y}_k^2 \rangle] \times \prod_{p \neq k} \left\{ \Gamma_{n,p}[\langle \tilde{y}_p^2 \rangle] \right\}} = \\ &\quad \frac{y_k}{\frac{\Gamma_{m,k}[\langle \tilde{y}_k^2 \rangle]}{\Gamma_{n,k}[\langle \tilde{y}_k^2 \rangle]} \times \prod_p \left\{ \Gamma_{n,p}[\langle \tilde{y}_p^2 \rangle] \right\}}, \end{aligned} \quad (7)$$

$$\text{式 中 : } \Gamma_{m,k}(\ast) = \sum_{m=0}^{\infty} \frac{(-1)^m}{m!(m+1)!} \left( \frac{1}{2} \right)^{2m} \left[ \frac{8}{g_k^2} (\ast) \right]^m;$$

$$\Gamma_{n,p}(\ast) = \sum_{n=0}^{\infty} \frac{(-1)^n}{n! n!} \left( \frac{1}{2} \right)^{2n} \left[ \frac{8}{g_p^2} (\ast) \right]^n.$$

由式(7)可知, 第  $k$  个信道理想中频信号  $\tilde{y}_k$  的求解

不仅依赖于  $y_k$ , 还依赖于各信道的理想中频信号, 所以无法直接计算得到。但可以将各信道进行联合处理, 通过迭代算法不断逼近  $\tilde{y}_k$ , 从而有效补偿非线性失真。整体的算法流程图如图2所示。第一次迭代将  $y_k$  作为相应信道  $\tilde{y}_k$  的估计  $y_{k,1}$ ,  $k=1, 2, \dots$ ; 首先将  $y_{k,1}$  在数字域平方并通过低通滤波得到  $\langle y_{k,1}^2 \rangle$ ; 然后分为两路: 一路

经过算子  $\Gamma_{n,k}(\cdot)$  处理并和其他信道经过算子  $\Gamma_{n,p}(\cdot)$  ( $p \neq k$ ) 处理的结果相乘得到  $z_1$ ; 另一路经过算子  $\Gamma_{m,k}(\cdot)$  处理并和本信道经过算子  $\Gamma_{n,k}(\cdot)$  处理的结果相除得到  $s_{k,1}$ ; 最后,  $y_k$  与  $z_1 \times s_{k,1}$  相除得到第一次迭代的结果。第二次迭代将每个信道第一次迭代的结果作为  $\tilde{y}_k$  的估计  $y_{k,2}$ , 重复上述过程。随后不断迭代, 逼近各信道接收的理想中频信号。

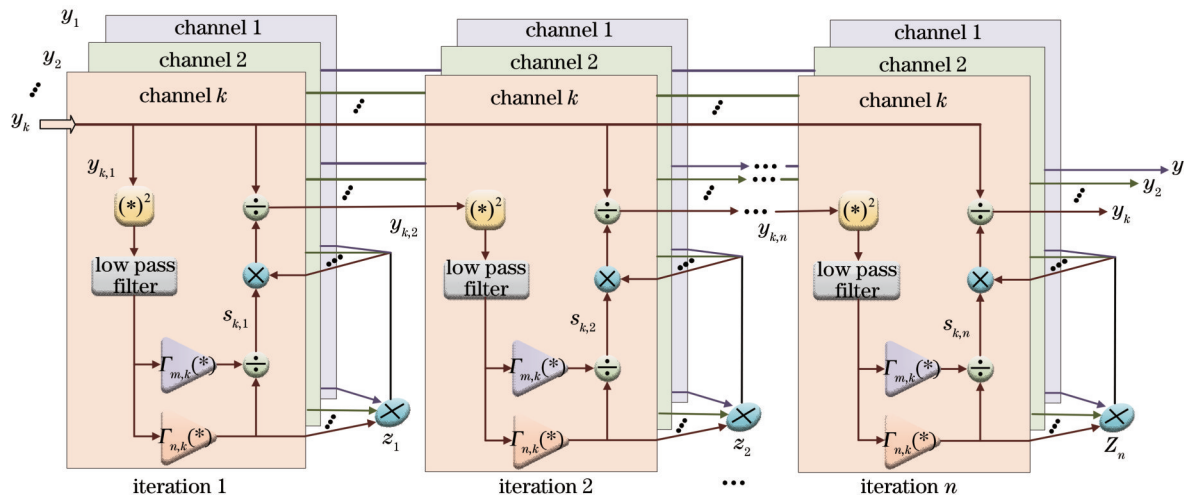


图2 数字非线性失真补偿算法流程图  
Fig. 2 Flow chart of digital nonlinear distortion compensation algorithm

### 3 结果与分析

用仿真软件 VPI transmission Maker 搭建了如图1所示的5通道微波光子信道化仿真系统。激光器输出的连续光波长为1550 nm, 功率为16 dBm。MZM的半波电压为5 V, 工作在正交偏置点。经过调制后的信号光被功分为5路, 分别用一个3 dB带宽、500 MHz的窄带光滤波器筛选出正一阶光边带。信道1至信道5的光滤波器中心频率与光载波的频率差分别为6、12.4、19.5、20.1、29.8 GHz。5个信道的本振光与光载波的频率差分别为5.04、11.44、18.54、19.14、

28.84 GHz; 每个信道宽带微波信号下变频的中心频率为960 MHz。平衡光电探测器(BPD)的响应度为1 A/W, 模数转换器(ADC)的有效位数为12 bit、采样率为4 GSa/s。

图3是输入两组双音信号下数字补偿前后的信号频谱。输入的双音信号分别为(5.995、6.005 GHz)和(12.397、12.403 GHz), 功率均为16 dBm。图3(a)是信道1输出信号的频谱。由图可见, 基频信号附近出现了由IMD3和XMD引入的频率分量。这些频率分量和基频信号的频率十分接近, 无法通过滤波直接去除。其中, XMD的功率为-61.27 dBm, IMD3的功率

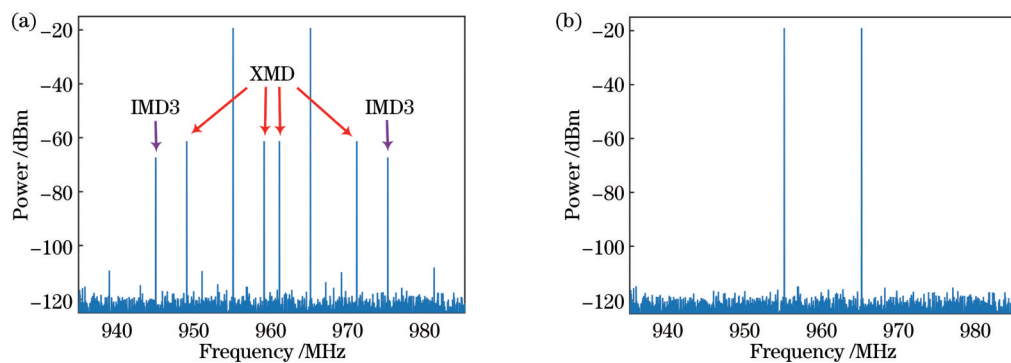


图3 数字补偿算法处理前后信道1信号的频谱。(a)处理前;(b)处理后

Fig. 3 Spectra of signals before and after processing by digital compensation algorithm in channel 1. (a) Before processing; (b) after processing

为 $-67.31\text{ dBm}$ 。经过本文提出的数字补偿算法处理后,信道1信号的频谱如图3(b)所示。与数字补偿算法处理前相比,IMD3和XMD被完全抑制在了噪声以下。进一步仿真表明,该数字补偿算法对其他信道的非线性失真具有相同的抑制效果。

图4给出了信道1中IMD3和XMD的功率随算法迭代次数的变化。由图可见,随着算法迭代次数的增加,IMD3和XMD的功率不断下降,只需要3到4次迭代便收敛,实现IMD3和XMD的同时补偿。表明该算法具有快速收敛能力。

图5给出了基频信号、IMD3和XMD的功率随着信道内双音信号功率和信道外双音信号功率的变化。输入的两组双音信号频率同上。图5(a)和5(b)对应信道外双音信号和信道内双音信号的功率分别固定为 $16\text{ dBm}$ 的情况。由图5(a)可见,随着信道内输入双音信号功率的增加,基频信号和XMD的功率以斜率为1的变化线性增加,IMD3的功率以斜率为3的变化线性增加。经过数字补偿算法处理后,IMD3和XMD都被抑制到噪声以下,且补偿的效果不会随着信道内双音

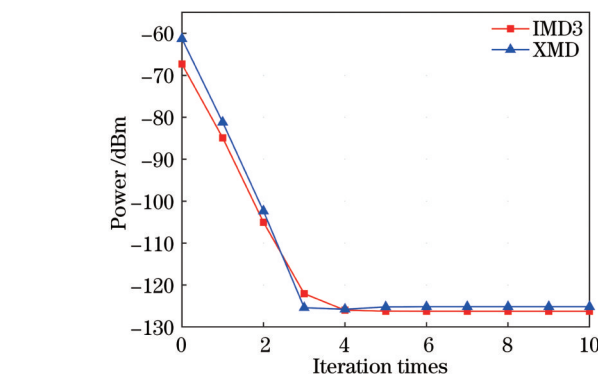
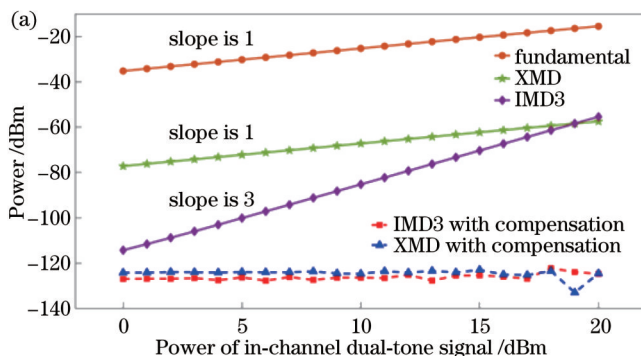


图4 IMD3和XMD的功率与算法迭代次数之间的关系

Fig. 4 Relationship between power of IMD3 and XMD and iteration times of algorithm

信号功率的增加而下降。同样地,固定信道内双音信号的功率为 $16\text{ dBm}$ ,如图5(b)所示。随着信道外输入双音信号功率的增加,基频信号和IMD3的功率不变,XMD的功率以斜率为2的变化线性增加,与理论预期一致<sup>[17]</sup>。在数字域完成补偿后,IMD3和XMD得到了完全抑制,都被抑制到了噪声以下。

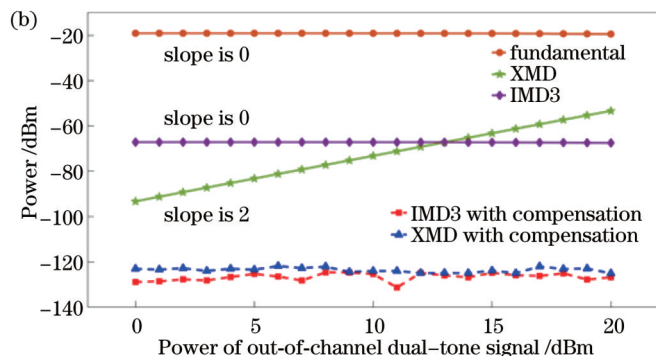


图5 基频信号、IMD3和XMD的功率随信道内外双音信号功率的变化。(a)信道内;(b)信道外

Fig. 5 Powers of fundamental signal, IMD3, and XMD varying with powers of in-channel dual-tone signal and out-of-channel dual-tone signal. (a) In-channel; (b) out-of-channel

图6为输入5组双音信号下数字补偿前后信号的频谱,以及参数偏差的影响。5组双音信号的频率分别为(5.999、6.001 GHz)、(12.421、12.43 GHz)、(19.549、19.5546 GHz)、(20.106、20.1094 GHz)、(29.831、29.839 GHz),功率均为 $15\text{ dBm}$ 。图6(a)显示了信道1输出信号的频谱,未经补偿前中频信号的非线性失真非常严重。由式(7)可知,该数字补偿算法依赖于各个信道的参数 $g_k(k=1, 2, \dots, 5)$ 。当各信道的参数 $g_k$ 都无偏差时,可以完全抑制该链路中的IMD和XMD,如图6(b)所示。当各信道的参数 $g_k$ 偏差都为5%时,数字补偿算法处理后该信道的频谱如图6(c)所示,IMD3和XMD分别抑制了 $15\text{ dB}$ 和 $16\text{ dB}$ 。图6(d)给出了IMD3和XMD抑制与参数偏差的关系,其中各信道参数 $g_k$ 的偏差相同。可见,随着

参数偏差的增大,IMD3和XMD的抑制效果不断下降,当参数偏差接近18%时,该算法对链路中非线性失真的抑制效果基本消失。

## 4 结 论

针对信道化相干探测链路中的IMD和XMD的问题,本文提出了一种基于数字域迭代的非线性失真补偿方法。该方法在后端数字信号处理模块对多个信道进行联合补偿,通过迭代不断逼近线性化的中频信号,能够同时抑制信道内的IMD和信道间的XMD,提高了微波光子信道化接收系统的线性度。仿真结果表明,在参数无偏差时,可以完全抑制IMD3和XMD;在参数偏差为5%时,仍可以使IMD3和XMD的抑制效果分别达到 $15\text{ dB}$ 和 $16\text{ dB}$ 。

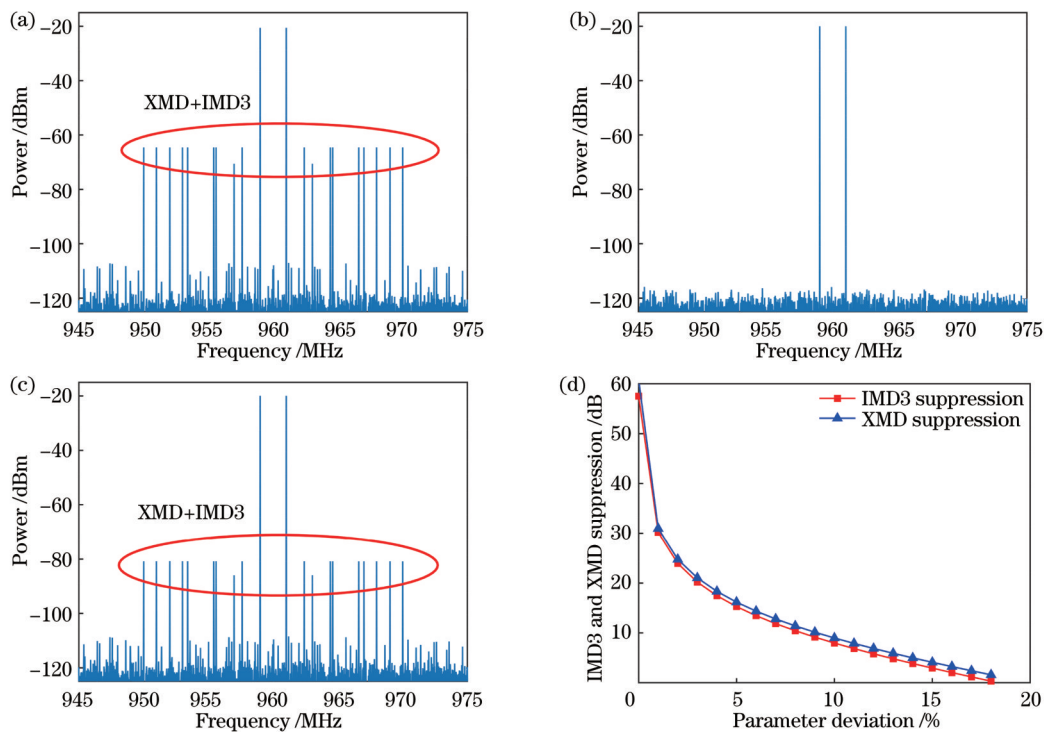


图6 输入5组双音信号下数字补偿前后信号的频谱和参数偏差的影响。(a)数字补偿算法处理前信号的频谱;(b)参数无偏差时数字补偿算法处理后信号的频谱;(c)参数偏差为5%时数字补偿算法处理后信号的频谱;(d)IMD3和XMD抑制与参数偏差的关系

Fig. 6 Spectra of signals before and after digital compensation under input of 5 sets of dual-tone signals and influence of parameter deviation. (a) Spectrum of signal before digital compensation algorithm processing; (b) spectrum of signal after digital compensation algorithm processing when parameter is accurate; (c) spectrum of signal after digital compensation algorithm processing when parameter deviation is 5%; (d) relationship between parameter deviation and suppression of IMD3 and XMD

## 参 考 文 献

- [1] Walden R H. Performance trends for analog to digital converters [J]. IEEE Communications Magazine, 1999, 37(2): 96-101.
- [2] Walden R H. Analog-to-digital converters and associated IC technologies[C]//2008 IEEE Compound Semiconductor Integrated Circuits Symposium, October 12-15, 2008, Monterey, CA, USA. New York: IEEE Press, 2008.
- [3] Hunter D B, Edvell L G, Englund M A. Wideband microwave photonic channelised receiver[C]//2005 International Topical Meeting on Microwave Photonics, October 14-14, 2005, Seoul, Korea (South). New York: IEEE Press, 2006: 249-252.
- [4] Xie X J, Dai Y T, Ji Y, et al. Broadband photonic radio-frequency channelization based on a 39-GHz optical frequency comb[J]. IEEE Photonics Technology Letters, 2012, 24(8): 661-663.
- [5] Wang S T, Sun Y W, Chen J P, et al. Broadband photonic RF channelization based on optical sampling pulse shaping[J]. IEEE Photonics Technology Letters, 2020, 32(18): 1195-1198.
- [6] Banwell T, Agarwal A, Toliver P, et al. Analytical expression for large signal transfer function of an optically filtered analog link [J]. Optics Express, 2009, 17(18): 15449-15454.
- [7] De Ridder R M, Korotky S K. Feedforward compensation of integrated optic modulator distortion[C]//Optical Fiber Communication, January 22, 1990, San Francisco, California. Washington, D.C.: Optica Publishing Group, 1990: WH5.
- [8] O'Connor S R, Clark J T R, Novak D. Wideband adaptive feedforward photonic link[J]. Journal of Lightwave Technology, 2008, 26(15): 2810-2816.
- [9] Katz A, Jemison W, Kubak M, et al. Improved radio over fiber performance using predistortion linearization[C]//IEEE MTT-S International Microwave Symposium Digest, June 8-13, 2003, Philadelphia, PA, USA. New York: IEEE Press, 2003: 1403-1406.
- [10] Magooon V, Jalali B. Electronic linearization and bias control for externally modulated fiber optic link[C]//International Topical Meeting on Microwave Photonics MWP 2000 (Cat. No.00EX430), September 11-13, 2000, Oxford, UK. New York: IEEE Press, 2002: 145-147.
- [11] Kim S K, Liu W, Pei Q B, et al. Nonlinear intermodulation distortion suppression in coherent analog fiber optic link using electro-optic polymeric dual parallel Mach-Zehnder modulator[J]. Optics Express, 2011, 19(8): 7865-7871.
- [12] Korotky S K, de Ridder R M. Dual parallel modulation schemes for low-distortion analog optical transmission[J]. IEEE Journal on Selected Areas in Communications, 1990, 8(7): 1377-1381.
- [13] Cui Y, Dai Y T, Yin F F, et al. Enhanced spurious-free dynamic range in intensity-modulated analog photonic link using digital postprocessing[J]. IEEE Photonics Journal, 2014, 6(2): 7900608.
- [14] Liu X, Liang X D, Dai Y T, et al. Suppression of nonlinear distortions in intensity modulated analog photonic link employing digital signal post-processing[C]//2016 IEEE International Topical Meeting on Microwave Photonics (MWP), October 31-November 3, 2016, Long Beach, CA, USA. New York: IEEE Press, 2016: 129-132.
- [15] Agarwal A, Banwell T, Toliver P, et al. Predistortion compensation of nonlinearities in channelized RF photonic links using a dual-port optical modulator[J]. IEEE Photonics Technology Letters, 2011, 23(1): 24-26.
- [16] Xie X J, Dai Y T, Xu K, et al. Digital joint compensation of IMD3 and XMD in broadband channelized RF photonic link[J].

- Optics Express, 2012, 20(23): 25636-25643.
- [17] Banwell T, Agarwal A, Toliver P, et al. Compensation of cross-gain modulation in filtered multi-channel optical signal processing applications[C]//Optical Fiber Communication Conference, March 21-25, 2010, San Diego, California. Washington, D.C.: Optica Publishing Group, 2010: OWW5.
- [18] Liu E J, Yu Z M, Yin C J, et al. Nonlinear distortions compensation based on artificial neural networks in wideband and multi-carrier systems[J]. IEEE Journal of Quantum Electronics, 2019, 55(5): 8000305.
- [19] Yin Y H, Yang W L, Xie S F, et al. High-efficiency mitigation of nonlinear distortion in microwave photonics link assisted by artificial neural network[J]. Wireless Communications and Mobile Computing, 2022, 2022: 1-8.
- [20] 刘育才. 动态信道化接收机设计与实现[D]. 成都: 成都理工大学, 2020: 5-14.  
Liu Y C. Design and implementation of dynamic channelized receiver[D]. Chengdu: Chengdu University of Technology, 2020: 5-14.

## Digital Compensation Method for Nonlinear Distortion of Microwave Photonic Channelized Link

Wang Jincheng, Chen Xiaoen, Ding Min, Chen Jianping, Wu Guiling\*

*State Key Laboratory of Advanced Optical Communication Systems and Networks, Shanghai Jiao Tong University, Shanghai 200240, China*

### Abstract

**Objective** Microwave photonic channelization technology converts broadband microwave signals to the optical domain for processing, breaking through the bandwidth limitations of conventional electronics. In general, external intensity modulation based on the Mach-Zehnder modulator (MZM) is employed in microwave photonic channelized links. However, due to the intrinsic cosine response of MZM, several nonlinear distortions occur in the process of electro-optical conversion, including harmonic distortion, intermodulation distortion (IMD), and cross-modulation distortion (XMD). Since the harmonic components can be effectively removed by filters, the IMD and XMD will become the main factors limiting the system's performance. Numerous electronic and optical methods have been proposed to compensate for the IMD in conventional narrow-band links, but they are incapable of suppressing the XMD. In this study, we propose a nonlinear distortion compensation scheme based on digital domain iteration processing, which can suppress the IMD and XMD simultaneously. Moreover, compared with the previous linearization methods, the proposed scheme does not require the construction of complex compensation function models or the introduction of additional hardware devices.

**Methods** Theoretical analysis shows that an approximate equation can be established between the distorted intermediate frequency signal output and the linear one from each channel. The iteration process can be utilized to approach the linearized output. Specifically, the distorted output in each channel can be selected as the initial value for the first iteration. The initial value is first squared and processed by low-pass filtering. Then, it is split into two paths that are processed by different operators. Finally, the results of the different channels processed by the operator are multiplied, and the distorted output is divided by them to obtain the result of the first iteration. Similarly, the output result of the first iteration can be used for the second iteration. Therefore, the digital compensation algorithm based on iteration can gradually convert the distorted output into a linear result.

**Results and Discussions** A simulation experiment is built to verify whether the simulation results are consistent with the theoretical derivation results. The signal spectra before and after the digital compensation algorithm processing are presented (Fig. 3). It can be found that rare times of iterations are sufficient to suppress the third-order intermodulation distortion (IMD3) and cross-modulation distortion (Fig. 4). With the increase in the fundamental signal power, the power of XMD and IMD3 increases with the slope of one and three, respectively [Fig. 5(a)]. As the power of the out-of-channel signal increases, the power of the fundamental signal and IMD3 is almost unchanged, while that of XMD increases with the slope of two [Fig. 5(b)]. According to the simulation experiment, the IMD3 and XMD can be completely suppressed [Fig. 6(b)] when the parameter is accurate. When the parameter deviation is 5%, IMD3 and XMD have been suppressed by 15 and 16 dB, respectively [Fig. 6(c)]. The ability of the digital compensation algorithm to suppress nonlinear distortion disappears as the parameter deviation approaches 18% [Fig. 6(d)].

**Conclusions** The linearity in microwave photonic channelized links is mainly limited by the IMD and XMD. In this study, a nonlinear distortion compensation method based on digital domain iteration processing is proposed, which jointly

processes the intermediate frequency signal output from each channel in the digital domain and approaches the ideal result of linearization through iteration. It can effectively suppress the IMD and XMD in channelized links. The simulation results show that the method can completely suppress the IMD and XMD when the parameter is accurate. When the parameter deviation is 5% , the IMD3 and XMD can still be suppressed by 15 and 16 dB , respectively.

**Key words** Fourier optics and signal processing; intermodulation distortion; cross-modulation distortion; microwave photon; digital signal processing